

Resonance Raman scattering studies of composition-modulated GaP/InP short-period superlattices

Hyeonsik M. Cheong, Yong Zhang, A. G. Norman, J. D. Perkins, and A. Mascarenhas
National Renewable Energy Laboratory, 1617 Cole Boulevard, Golden, Colorado 80401

K. Y. Cheng and K. C. Hsieh

Department of Electrical and Computer Engineering, University of Illinois at Urbana-Champaign, Urbana, Illinois 61801

(Received 28 December 1998)

Resonance Raman scattering and electroreflection measurements on laterally composition modulated GaP/InP short-period superlattices are presented. The electroreflectance spectra give the fundamental band-gap energy of the lateral superlattice at 1.69 ± 0.05 eV, which is about 210 meV lower than the band-gap energy of a GaInP random alloy with the same overall composition. In resonance Raman spectra measured with the polarization of both excitation and scattered photons along the composition modulation direction, the GaP-like longitudinal optical phonon redshifts by 4.0 ± 0.5 cm^{-1} near the resonance with the fundamental energy gap. A comparison of the experimental data with a model calculation gives the average In composition in the In-rich region as 0.70 ± 0.02 , and the average Ga composition in the Ga-rich region as 0.68 ± 0.02 .

[S0163-1829(99)04531-2]

I. INTRODUCTION

Spontaneous lateral composition modulation (CM) in III-V alloys and short-period superlattices (SPS's) grown by molecular beam epitaxy (MBE) or organometallic vapor phase epitaxy has been studied extensively in recent years.¹⁻⁷ This phenomenon has been observed in $\text{Ga}_x\text{In}_{1-x}\text{As}$ and $\text{Al}_x\text{In}_{1-x}\text{As}$ alloys; and GaP/InP, GaAs/InAs, and AlAs/InAs SPS's. For example, when a $(\text{GaP})_2/(\text{InP})_2$ SPS was grown by MBE on a (001) GaAs substrate, it was found that the cation composition is modulated along the [110] direction with a periodicity of ~ 100 – 200 Å: here each GaP (InP) layer is transformed into a $\text{Ga}_{1-x}\text{In}_x\text{P}(\text{Ga}_{1-y}\text{In}_y\text{P})$ layer where the $x(y)$ value oscillates along the [110] direction. The result is a lateral superlattice with alternating (110) layers of Ga-rich and In-rich material.¹ This is schematically illustrated in Fig. 1: the vertically averaged composition is modulated along the [110] direction, while a vestige of the SPS structure remains.⁸ The interplay between the composition modulation wave and the concomitant coherency strain wave results in a lateral superlattice that has a band-gap energy much lower than that of the random alloy with the same overall average composition, and the band-edge luminescence shows a strong anisotropy that is attributable to a lateral superlattice effect.^{3,7} This phenomenon has been utilized to grow multiple-quantum-wire lasers with enhanced performance characteristics.⁹

In understanding the effect of the CM phenomenon on the materials properties of alloys and SPS's, it is critical to know the actual extent of the composition variation. Energy-dispersive x-ray microanalysis has been used to estimate the variation of the local composition,^{1,10} but this technique requires special sample preparation that does not preserve the integrity of the samples. Estimating the composition variation by comparison of the superlattice band-gap energy measured with optical techniques such as photoluminescence or modulation spectroscopy with that obtained from theoretical

calculations usually does not yield a unique solution because many input parameters remain unknown.

Raman scattering measurements can be used to estimate the average composition of bulk alloys by comparing the measured phonon frequencies with the known composition dependence of phonon frequencies.^{11,12} Furthermore, microscopic fluctuations of alloy concentrations can be estimated by monitoring the phonon frequencies near resonances in resonance Raman scattering measurements. Sela *et al.* used this technique to probe composition fluctuations in the length scale of ~ 50 Å in $\text{Al}_x\text{Ga}_{1-x}\text{As}$ and $\text{Ga}_x\text{As}_{1-x}\text{P}$ alloys.^{13,14} This technique can be applied to the composition modulated lateral superlattice to estimate the composition variation by providing extra input in addition to the superlattice band-gap energy that is obtained from photoluminescence or modulation spectroscopy. For example, when the excitation laser energy is tuned away from resonances (*off-resonance*), the

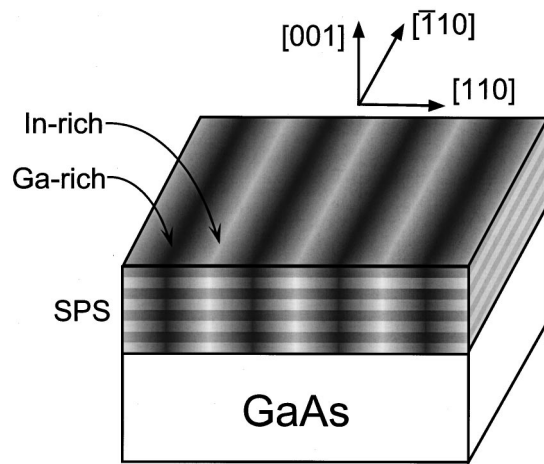


FIG. 1. Schematic illustration of the sample structure. $(\text{GaP})_{2,2}/(\text{InP})_2$ SPS grown on a GaAs buffer layer results in composition modulation in the [110] direction.

Raman spectrum of a composition modulated GaP/InP SPS should comprise signals from the Ga-rich as well as the In-rich regions of the sample. However, if the laser energy is tuned to be resonant with the fundamental band gap of the lateral superlattice, the Raman scattering signal should come predominantly from the In-rich region, because the ground-state electron and hole wave functions are both localized in that region, and so the optical transitions occur in the In-rich region. Consequently, the phonon frequencies would redshift towards those for In-rich compositions near the resonance. Thus, the phonon frequency shift near the resonance is a good measure of composition and strain in the In-rich region. Since the local coherency strain in the In-rich region depends on the composition in the Ga-rich region as well as that in the In-rich region, one can estimate the compositions in the In-rich region and in the Ga-rich region simultaneously, by comparing the phonon frequency shift with the superlattice band-gap energy.

Recently, resonance Raman scattering was used to estimate the alloy composition fluctuation in composition modulated lateral superlattices. However, in this earlier work,¹⁵ the polarizations of the excitation laser or the scattered photons were not specified, and the effect of the coherency strain was neglected in the analysis. As will be shown later, it turns out that the resonance behavior of the phonons is strongly dependent on the polarizations of the probing photons, and therefore, important details are obscured in *unpolarized* studies. In this paper, we combine *polarized* electroreflectance with *polarized* resonance Raman scattering measurements to estimate the average alloy compositions in the Ga-rich and In-rich regions of composition modulated GaP/InP SPS layers.

II. EXPERIMENT

The samples were grown by a single-step gas source MBE process on (001)-oriented, on-axis semi-insulating GaAs substrates. Elemental Ga and In sources were used for group III fluxes, while P₂ cracked from phosphine was used as the group V flux. The substrate temperature was kept at ~530 °C with a growth rate of ~1 μm/hr, as calibrated by reflection high-energy electron diffraction intensity oscillation measurements. The layer structure consists of a 0.2 μm undoped GaAs buffer layer, followed by 80 pairs of (GaP)_{2.2}/(InP)₂ short-period superlattice (SPS) layer. The thickness ratio of the GaP and InP layers, 2.2/2.0, gives an overall composition of Ga_{0.52}In_{0.48}P, which is nominally lattice matched to the GaAs substrate.

The room-temperature polarized electroreflectance (ER) spectra were measured using a contactless electroreflectance technique¹⁶ where the sample is mounted between two parallel conducting planes as in a parallel plate capacitor. A SnO₂-coated glass slide provides the transparent front conducting plane necessary to enable reflection measurements in the presence of a modulating electric field. The polarized electroreflectance spectra were measured in a near-normal incidence geometry using a scanning monochromator with a broad-band tungsten-filament bulb as a light source. The polarized probe beam was focused to a ~0.5 mm×2 mm spot on the sample and the reflected light was refocused into a Si photodiode detector. A lock-in amplifier was used to mea-

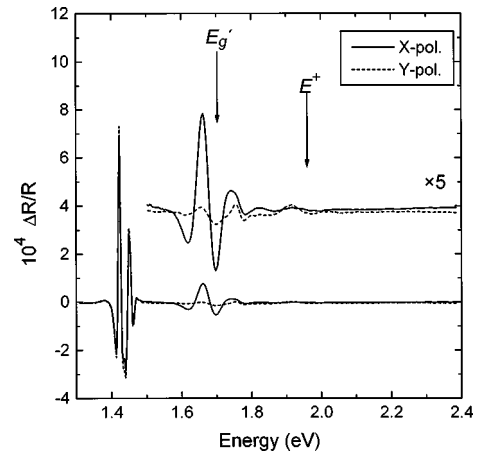


FIG. 2. Polarized electroreflectance spectra taken with the polarization orthogonal (*X*) and parallel (*Y*) to the CM direction [110]. The signal at ~1.69 eV comes from the band gap of the lateral superlattice. The expanded higher energy portions show additional transitions at higher energies.

sure the change in reflectance due to a modulating voltage of ±750 volts at 400 Hz. Properly normalized $\Delta R/R$ spectra are obtained by simply dividing the modulated signal by the dc signal. The spectral resolution was 3 nm, or 7 meV at 1.7 eV.

Resonance Raman scattering measurements were performed at room temperature in a quasibackscattering geometry. The excitation source was either a Ti:sapphire laser (1.58-1.82 eV) or a dye laser with Rhodamine 6G dye (1.94-2.17 eV). 100 mW of the excitation laser beam was focused with a cylindrical lens to a line of dimensions 5 mm × 100 μm. The scattered photons were dispersed by a SPEX 1877 0.6-m triple spectrometer and detected by a liquid-nitrogen-cooled charge coupled device detector array. The spectral resolution was about 2 cm⁻¹. In order to measure the phonon-peak positions accurately, we calibrated the spectra using the frequency of the longitudinal optical phonon peak (292 cm⁻¹) of the GaAs substrate.¹⁷ The *absolute* accuracy of this frequency calibration is about ±1 cm⁻¹ due to the scatter in the GaAs LO phonon frequency data found in the literature, but the *relative* accuracy between our spectra is estimated to be better than ±0.5 cm⁻¹.

III. RESULTS

(002) dark-field transmission-electron-microscopy images taken in ($\bar{1}10$) cross section shows alternating bright and dark contrast, corresponding to In-rich and Ga-rich regions,¹ along the [110] direction with a period of ~120–150 Å. We take the average period of the CM wave to be 135 ± 15 Å. No lateral contrast variation is observed in the (110) cross section. Figure 2 shows two ER spectra taken with the polarization aligned along the $[\bar{1}10]$ and [110] directions. Here, we take $X = [\bar{1}10]$, $Y = [110]$, and $Z = [001]$. The sharp feature near 1.42 eV is due to the GaAs substrate. The broad feature near 1.69 eV is due to the optical transition across the fundamental band gap E_g' of the lateral superlattice in the SPS layer. This feature shows a strong polarization anisotropy: the signal is much stronger in the *X* polarization than in the *Y*

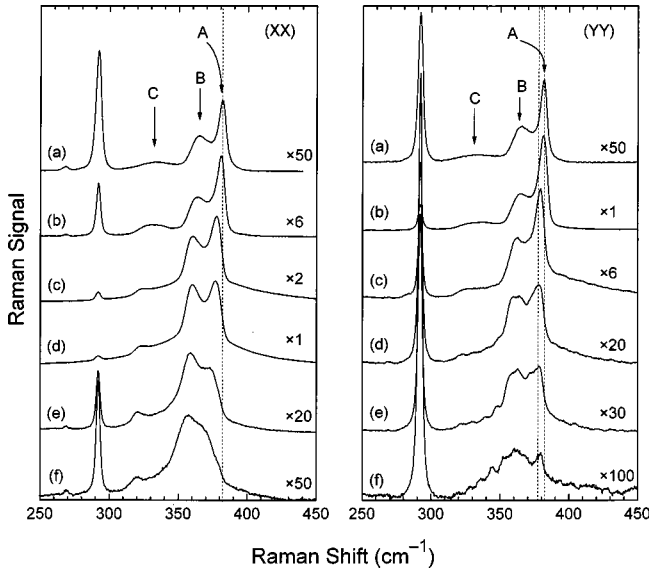


FIG. 3. Series of polarized Raman spectra for (XX) and (YY) polarizations, where polarizations of the excitation laser and the scattered photons are both along the X or Y direction, respectively. The excitation energies are: (a) 2.410, (b) 2.008, (c) 1.768, (d) 1.712, (e) 1.625, and (f) 1.602 eV for the (XX) polarization; and (a) 2.410, (b) 2.008, (c) 1.789, (d) 1.696, (e) 1.668, and (f) 1.602 eV for the (YY) polarization. Each series is separately normalized with the factors on the right.

polarization. This polarization anisotropy is a direct result of the lateral superlattice effect: if the structure were a perfect lateral superlattice with the superlattice axis along the Y direction, the lowest-energy optical transition would be forbidden for the Y polarization.¹⁸ Since the lateral superlattice is not perfect, and a vestige of the vertical SPS persists,⁷ a finite signal is observed even in the Y polarization. The broad linewidth of this feature reflects the imperfect periodicity of the CM wave and the possibility that the amplitude of the CM is not uniform throughout the sample. From these spectra, the superlattice band-gap energy E'_g is determined to be 1.69 ± 0.05 eV, which represents a 210 meV redshift relative to the band-gap energy of the random alloy whose average Ga composition is 0.52. These results are similar to those obtained from earlier polarized photoreflectance measurements.³ In addition, closer inspection of the expanded spectra indicates that there are additional spectral features at higher energies up to ~ 2.05 eV. We attribute these features to higher-energy transitions of the lateral superlattice. The strongest of these higher-energy features is the one at 1.9–2.0 eV, marked E^+ . This one appears stronger in the Y polarization than in the X polarization, which is opposite to the behavior of the feature near 1.69 eV attributed to the lowest-energy transition of the lateral superlattice. This difference will be discussed in the next section.

Figure 3 shows two series of Raman spectra taken in a quasibackscattering geometry with (XX) and (YY) polarizations, where (XX) , for example, refers to a configuration with polarizations of both the excitation and scattered photons aligned along the X direction. The “off-resonance” spectra (the top spectrum of each series), taken with the 5145-Å line of an Ar-ion laser as the excitation source, are similar to that of a typical random alloy $\text{Ga}_{0.52}\text{In}_{0.48}\text{P}$:¹⁹ a sharp GaP-like

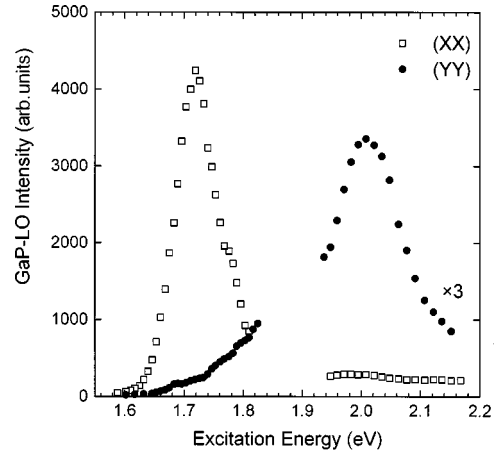


FIG. 4. Intensity of the GaP-like LO phonon peak as a function of the excitation energy. A strong resonance at ~ 1.72 eV is seen for the (XX) polarization. This resonance is much weaker for the (YY) polarization. At ~ 2.0 eV, a moderately strong resonance for the (YY) polarization and a weak resonance for the (XX) polarization are seen.

longitudinal optical (LO) phonon peak at 381.8 cm^{-1} (A), a relatively broader InP-like LO phonon peak at $\sim 364 \text{ cm}^{-1}$ (B), and a weak and broad transverse optical (TO) phonon peak at $\sim 330 \text{ cm}^{-1}$ (C) are observed. In addition, an LO phonon peak at 292 cm^{-1} and a much weaker TO phonon peak at 269 cm^{-1} from the GaAs substrate are seen. In the (XX) polarization, as the excitation energy is lowered, the Raman spectrum changes dramatically. All three phonon peaks A , B , and C move toward lower frequencies. In addition, the intensity of the InP-like LO phonon peak (B) increases relative to that of the GaP-like LO phonon peak (A) with decreasing excitation energy and the peak A becomes unresolved at the lowest excitation energies. On the other hand, in the (YY) polarization, the changes are less dramatic. The phonon peaks redshift initially with decreasing excitation energies, but blueshift back toward the “off-resonance” frequencies as the excitation energy is lowered below ~ 1.7 eV. Also, the InP-like LO phonon peak B does not completely dominate the spectrum as in the (XX) polarization at the lowest excitation energies, but the GaP-like LO phonon peak A is always resolved. We note that the signal-to-noise ratio of the spectra is significantly lower for the lower excitation energies in this polarization due to the much weaker signals (see Fig. 4).

In order to examine the dependence of the Raman spectra on the excitation energy, we have analyzed the intensity and the frequency of the GaP-like LO phonon peak A in detail. A similar analysis can be done for the InP-like LO phonon peak B , but the broad linewidth of the peak B would result in much larger uncertainties. Since the total thickness of the SPS layer is only 100 nm, we ignored the absorption effect. Figure 4 plots the intensity of the GaP-like LO phonon peak as a function of the excitation energy for the two polarizations. At ~ 1.72 eV, near the superlattice band-gap energy E'_g observed in the ER measurement, a strong resonance is observed in the (XX) polarization.²⁰ In the (YY) polarization, on the other hand, this resonance is very much weaker, and occurs at 1.69 eV. This polarization dependence is consistent with what is observed in the ER measurements. Near 2.0 eV,

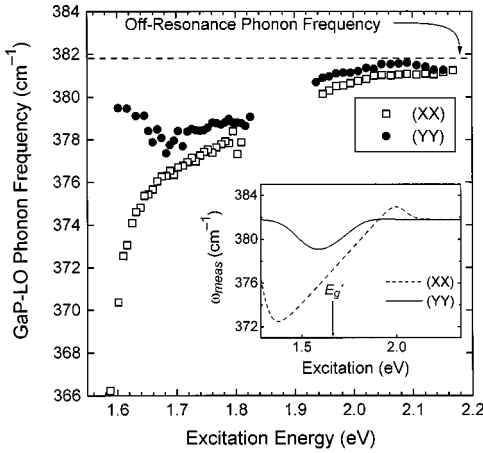


FIG. 5. Frequency of the GaP-like LO phonon as a function of the excitation energy. In the (XX) polarization, the phonon frequency varies monotonically with the excitation energy. At the lowest excitation energy measured, the phonon frequency is lower by $\sim 16 \text{ cm}^{-1}$ relative to the “off-resonance” frequency. In the (YY) polarization, the phonon shifts $\sim 4 \text{ cm}^{-1}$ towards lower frequency near the resonance at $\sim 1.69 \text{ eV}$. [Inset: Comparison of the dependence of the phonon frequency on the excitation energy, calculated using Eq. (1). The plots reproduce the difference in the excitation dependence of the phonon frequency between the two polarizations observed in the experimental data].

a moderately strong resonance is observed for the (YY) polarization, while a weaker resonance is seen for the (XX) polarization. We attribute this resonance to the higher-energy transition E^+ observed in the ER spectra. The polarization behavior is consistent with the ER spectra that show a stronger signal in the Y polarization in this energy range. We checked for additional resonances between 1.82 and 1.94 eV and observed no other resonance in either polarization. In Fig. 5, the excitation-energy dependence of the frequency of the GaP-like LO phonon peak A is plotted for the two polarizations. In the (XX) polarization, the GaP-like LO phonon peak A shifts to lower energy monotonically as the excitation energy is lowered, as seen earlier in Fig. 3. In this polarization, for the lowest excitation energies where the peak A is not resolved in the spectrum (see Fig. 3), its peak frequency was extracted from a double-Lorentzian fit of the portion of the spectrum that contains both the peaks A and B . At 1.72 eV, where the phonon intensity is maximum, the phonon frequency is $4.5 \pm 0.5 \text{ cm}^{-1}$ lower than the “off-resonance” phonon frequency of 381.8 cm^{-1} . As the excitation energy is lowered further, the phonon peak moves further toward lower frequencies, and at the lowest excitation energy used (1.59 eV), this phonon peak redshifts by almost 16 cm^{-1} relative to the “off-resonance” phonon frequency. In the (YY) polarization, the phonon peak frequency reaches a minimum near 1.69 eV, where it is lower by $4.0 \pm 0.5 \text{ cm}^{-1}$ relative to the off-resonance frequency. At lower energies, the peak blueshifts as the excitation energy is further lowered.

IV. DISCUSSION

The striking difference between the two polarizations as regards the behavior of the excitation-energy dependence of the GaP-like LO phonon frequency is intriguing. The excita-

tion dependence of the phonon frequency in the (YY) polarization is consistent with the scenario presented in the introduction: the phonon frequency is similar to that of a random alloy with the same overall composition when the excitation energy is away from the resonance, but is redshifted near the resonance at 1.69 eV. On the other hand, the excitation dependence of the phonon frequency in the (XX) polarization is anomalous in that even at low-excitation energies the phonon frequency decreases monotonically as the excitation energy is lowered, i.e., moved away from the resonance. This anomaly results from the inhomogeneity of the sample and the very strong resonance effect in this polarization. Since the period and the amplitude of CM are not uniform throughout the sample, there exist regions where the *local* In concentration is higher than the *average* In concentration of all the In-rich regions, $\langle x_{\text{In}} \rangle$. In these regions, the resonance occurs at a *local band-gap energy* that is lower than the spatially averaged band gap E_g' of 1.69 eV. When the excitation laser energy is in resonance with the *local* band gap of these regions, the Raman spectrum would be dominated by contributions from these regions due to the strong resonance in this polarization, and consequently, the phonons redshift to reflect the higher In content in these regions. As the excitation energy is further lowered, the volume fraction of such regions where the local band-gap energy is in resonance with the excitation becomes very small, but the Raman contribution from these small volumes is still larger than that from the rest of the sample due to the strong resonance effect. This can be explained in a simplified model as follows. If we assume that the local band-gap energy has a distribution function $f(E)$, the measured phonon frequency ω_{meas} for an excitation energy E_{ex} can be written as a weighted average of two contributions

$$\omega_{\text{meas}}(E_{\text{ex}}) = [1 + |Cf(E_{\text{ex}})|^2]^{-1/2} \times [\omega_{\text{nr}}^2 + |Cf(E_{\text{ex}})\omega_r(E_{\text{ex}})|^2]^{1/2}, \quad (1)$$

where ω_{nr} is the “nonresonant” phonon frequency (318.8 cm^{-1}), $\omega_r(E)$ the phonon frequency of the material that has a band gap of E , C a constant that represents the strength of the resonance. For excitations away from the resonance, $f(E_{\text{ex}}) \sim 0$, and thus $\omega_{\text{meas}} \sim \omega_{\text{nr}}$. Using this formalism and assuming that $\omega_r(E)$ is a linear function of E and that C is 20 times stronger for the (XX) polarization than for the (YY) polarization, we obtained the curves in the inset of Fig. 5 that reproduce the major difference between the two polarizations as observed in the experimental data of Fig. 5.

This interpretation is supported by the fact that even at the lowest excitation energies, the Raman signal is significantly stronger in the (XX) polarization than in the (YY) polarization. It is also consistent with the changes in the shape of the Raman spectrum at lowest excitation energies, where the InP-like LO phonon becomes stronger than the GaP-like LO phonon, indicating that the signal is coming from very In-rich material. Within this interpretation, the volume fraction of these extra-In-rich regions can be inferred from the resonance plot of Fig. 4. For example, at the lowest excitation energy used, the phonon intensity is about 1% of that at the

peak of the resonance. From this, one can infer that the very In-rich regions that yield a 16-cm^{-1} redshift of the GaP-like LO phonon occupy a small fraction on the order of 1% of the total sample volume.

On the other hand, the resonance behavior in the (YY) polarization is governed primarily by the fact that since the resonance is weak in this polarization, the scattering intensity is determined by the regions with In concentrations close to $\langle x_{\text{In}} \rangle$, i.e., by the volume distribution of the In-rich regions, where $\langle x_{\text{In}} \rangle$ is the spatial average of the In concentration for all the In-rich regions. Therefore, we take $-4.0 \pm 0.5 \text{ cm}^{-1}$ as the average phonon frequency shift of the GaP-like LO phonon that occurs due to the high In-concentration of the In-rich regions. In contrast, there is no comparable blueshift of the phonons in either polarization near the resonance at $\sim 2.0 \text{ eV}$. The reason for this is as follows: for the lowest-energy transition, both the electron and hole wave functions are localized in the In-rich regions and thus the contribution to the Raman signal comes predominantly from the In-rich region when the excitation is in resonance with this critical point. In contrast, the electron and hole wave functions for the higher-energy states are not as strongly localized within the In-rich region. In fact, our calculations⁷ show that the electron and hole states that are involved in the transition E^+ have wave functions that are significantly delocalized between the Ga- and In-rich regions. Therefore, Raman scattering near this resonance probes both the Ga- and In-rich regions simultaneously and no major shift in the phonon frequency is expected. This is consistent with previous resonance Raman measurements on $\text{Al}_x\text{Ga}_{1-x}\text{As}$ alloys, where only Ga-rich regions could be detected.¹⁴

One can estimate the average In and Ga concentration in the In- and Ga-rich regions, $\langle x_{\text{In}} \rangle$ and $\langle x_{\text{Ga}} \rangle$, respectively, from the knowledge of: the period of the CM wave $135 \pm 15 \text{ \AA}$; the average phonon shift $\delta\omega$ of GaP-like LO phonon, $-4.0 \pm 0.5 \text{ cm}^{-1}$; and the average superlattice band-gap energy E'_g of $1.69 \pm 0.05 \text{ eV}$. Since both $\delta\omega$ and E'_g are functions of composition as well as the lateral coherency strain, which in turn is determined by the lateral composition variation, we estimated $\langle x_{\text{In}} \rangle$ and $\langle x_{\text{Ga}} \rangle$ by simultaneously fitting the phonon-frequency shift and E'_g to a model calculation. We assume that the CM layer is strained in the [110] direction as discussed by Glas who determined that when the thickness of a composition modulated layer is larger than the period of the modulation, as in our case, the coherency strain is tetragonal in the CM direction.²¹ The strength of the lateral coherency strain in each In- or Ga-rich layer is then determined by the amplitude of the lateral composition modulation wave in each layer and the ratio of the width of the In-rich layer to that of the Ga-rich layer. Since the overall composition should be $\text{Ga}_{0.52}\text{In}_{0.48}\text{P}$, the width ratio is constrained by the amplitude of the lateral composition modulation wave in each layer. We assume that the composition modulation wave has an asymmetric sinusoidal form, i.e., it is sinusoidal in both the Ga- and In-rich regions but the amplitude and the period are different, as illustrated in Fig. 6. The amplitude of the sinusoidal variation is larger than δx_{In} and δx_{Ga} by a factor of $\pi/2$, where $\delta x_{\text{In}} = \langle x_{\text{In}} \rangle - 0.48$ and $\delta x_{\text{Ga}} = \langle x_{\text{Ga}} \rangle - 0.52$, respectively. First, the dependence of $\delta\omega$ on δx_{In} and δx_{Ga} is calculated using the deformation potentials found in the literature,²² and the result is plotted in Fig.

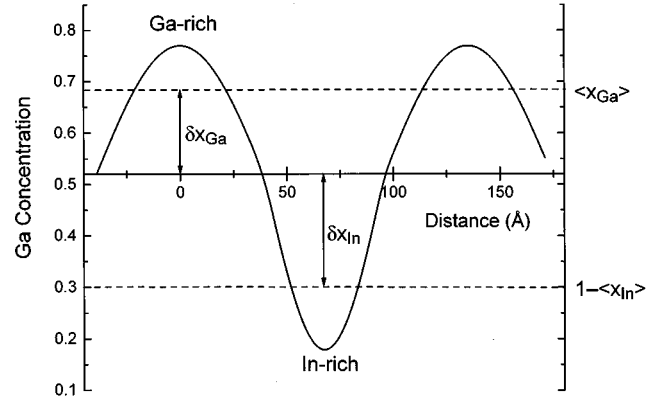


FIG. 6. Asymmetric sinusoidal profile of the composition variation used in our model calculation.

7. Then, for those pairs of δx_{In} and δx_{Ga} values that are consistent with the observed $\delta\omega$ of $-4.0 \pm 0.5 \text{ cm}^{-1}$, we calculated the superlattice band-gap energy E'_g using the method described in Ref. 7. In this calculation, the effects of the vertical SPS modulation as well as the lateral CM modulations are included. The best fit to the experimental values of $\delta\omega$ and E'_g is obtained for $(\delta x_{\text{In}}, \delta x_{\text{Ga}}) = (0.22, 0.16)$ with an uncertainty of ± 0.02 . This translates into $\langle x_{\text{In}} \rangle = 0.70 \pm 0.02$ and $\langle x_{\text{Ga}} \rangle = 0.68 \pm 0.02$. In the above analysis, we used simple sinusoidal averages $\langle x_{\text{In}} \rangle$ and $\langle x_{\text{Ga}} \rangle$ to calculate the phonon shifts. Since the phonon shift is not very sensitive on δx_{In} in the range that we are interested, we believe using a wave function-weighted average instead of the simple average would not significantly affect the results. These results compare with $\langle x_{\text{In}} \rangle = 0.56$ and $\langle x_{\text{Ga}} \rangle = 0.58$ found from energy dispersive x-ray microanalysis on earlier samples.¹ Our model calculation also shows that the third electron state and the fifth hole state are the lowest-energy *delocalized* states in the respective bands and the optical transition between these states occurs at $\sim 2.05 \text{ eV}$. This transition exhibits the same polarization as the feature labeled E^+ in the ER spectra (Fig. 2). We interpret this tran-

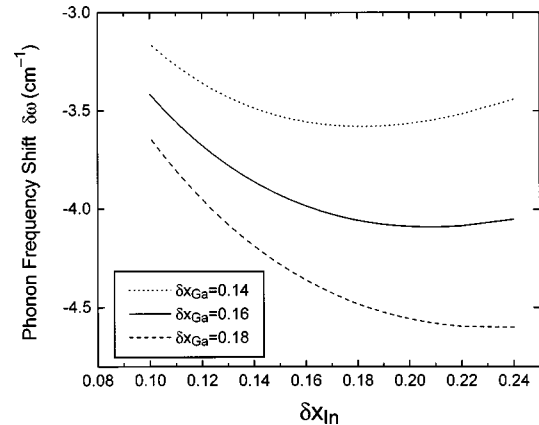


FIG. 7. Dependence of the phonon-frequency shift on the composition variation. Here, $\delta x_{\text{In}} = \langle x_{\text{In}} \rangle - 0.48$ and $\delta x_{\text{Ga}} = \langle x_{\text{Ga}} \rangle - 0.52$, where $\langle x_{\text{In}} \rangle$ is the average In composition in the In-rich regions and $\langle x_{\text{Ga}} \rangle$ the average Ga composition in the Ga-rich regions.

sition to correspond to the resonance near 2.0 eV observed in Fig. 4. The small disagreement between the calculated and observed energies for this transition is not unreasonable because the uncertainty in the estimate of the excited-state energies is usually much larger than that for the lowest energy states.

It appears that the maximum phonon shift of 16 cm^{-1} in the (*XX*) polarization that we earlier interpreted as arising from small volumes with excessively high-In compositions is inconsistent with this result, because a simple extrapolation would give x_{In} in such regions to be in excess of 1. However, it should be remembered that the above analysis assumes that the regions under consideration are coherently strained along the [110] direction. If the strain is locally relaxed, the same phonon shift would correspond to a much smaller composition amplitude swing δx_{In} . For such extremely In-rich regions, the strain is likely to be incoherent because of the high elastic strain energy involved. For the case where the strain is fully relaxed, a 16 cm^{-1} phonon shift corresponds to a composition amplitude swing $\delta x_{\text{In}}=0.25$, or $x_{\text{In}}=0.73$, which is the lower bound for the In-composition in such excessively In-rich regions. In real situations, it is likely that the strain is partially relaxed, and therefore, x_{In} could be significantly large than this lower bound.

V. CONCLUSION

We have performed resonance Raman scattering and electroreflection measurements on laterally composition modulated GaP/InP short-period superlattices. The electroreflectance spectra give the fundamental band-gap energy of the lateral superlattice. In resonance Raman spectra in the (*YY*) polarization, the GaP-like phonon redshifts by $4.0 \pm 0.5 \text{ cm}^{-1}$ near the resonance with the fundamental energy gap. On the other hand, the resonance Raman spectra in the (*XX*) polarization are dominated by a strong resonance effect and indicate that there are small volumes (less than 1% volume fraction) where the composition is excessively In-rich. By fitting the results of a model calculation with the experimental data it is estimated that the average In concentration in the In-rich region is 0.70 ± 0.02 , and the average Ga concentration in the Ga-rich region is 0.68 ± 0.02 .

ACKNOWLEDGMENTS

We thank F. Alsina for helpful discussions. The work at NREL was supported by the Office of Science (Materials Sciences Division) of the Department of Energy under Contract No. DE-AO36-83CH10093. The work at the University of Illinois was supported by the National Science Foundation and the Joint Services Electronics Program.

-
- ¹K. C. Hsieh, J. N. Baillargeon, and K. Y. Cheng, *Appl. Phys. Lett.* **57**, 2244 (1990).
- ²K. Y. Cheng, K. C. Hsieh, and J. N. Baillargeon, *Appl. Phys. Lett.* **60**, 2892 (1992).
- ³A. Mascarenhas, R. G. Alonso, G. S. Horner, S. Froyen, K. C. Hsieh, and K. Y. Cheng, *Superlattices Microstruct.* **12**, 57 (1992).
- ⁴A. Mascarenhas, R. G. Alonso, and G. S. Horner, S. Froyen, K. Y. Cheng, *C. Rev. B* **48**, 4907 (1993).
- ⁵S. W. Jun, T.-Y. Seong, J. H. Lee, and B. Lee, *Appl. Phys. Lett.* **68**, 3443 (1996).
- ⁶J. Mirecki Millunchick, R. D. Twisten, S. R. Lee, D. M. Follstaedt, E. D. Jones, S. P. Ahrenkeif, Y. Zhang, H. M. Cheng, and A. Mascarenhas, *J. Electron. Mater.* **26**, 1048 (1997).
- ⁷Y. Zhang and A. Mascarenhas, *Phys. Rev. B* **57**, 12 245 (1998).
- ⁸See Ref. 7 for a detailed description.
- ⁹S. T. Chou, K. Y. Cheng, L. J. Chou, and K. C. Hsieh, *Appl. Phys. Lett.* **66**, 2220 (1995).
- ¹⁰D. M. Follstaedt, R. D. Twisten, J. M. Millunchick, S. R. Lee, E. D. Jones, S. P. Ahrenkeif, Y. Zhang, and A. Mascarenhas, *Physica E* **2**, 325 (1998).
- ¹¹B. Jusserand and S. Slempek, *Solid State Commun.* **49**, 95 (1984).
- ¹²T. Kato, T. Matsumoto, and T. Ishida, *Jpn. J. Appl. Phys., Part 1* **27**, 983 (1988).
- ¹³I. Sela, V. V. Gridin, R. Beserman, R. Sarfaty, D. Fekete, and H. Morkoç, *J. Appl. Phys.* **63**, 966 (1988).
- ¹⁴I. Sela, V. V. Gridin, R. Beserman, and H. Morkoç, *Phys. Rev. B* **37**, 6393 (1988).
- ¹⁵P. Dua, L. Cooper, and K. Y. Cheng, *Appl. Phys. Lett.* **72**, 1072 (1998).
- ¹⁶X. Yin and F. H. Pollak, *Appl. Phys. Lett.* **59**, 2305 (1991).
- ¹⁷J. S. Blakemore, *J. Appl. Phys.* **53**, R123 (1982).
- ¹⁸G. Bastard, *Wave Mechanics Applied to Semiconductor Heterostructures* (Les Éditions de Physique, Les Ulis, 1988).
- ¹⁹H. M. Cheong, A. Mascarenhas, P. Ernst, and C. Geng, *Phys. Rev. B* **56**, 1882 (1997).
- ²⁰The maximum Raman intensity occurs at an excitation energy ($\sim 1.72 \text{ eV}$) slightly higher than the critical point measured by CER ($\sim 1.69 \text{ eV}$). Such a small shift is common in resonance Raman spectroscopy. [M. Cardona, in *Light Scattering in Solids*, edited by M. Cardona and G. Güntherodt (Springer-Verlag, Berlin, 1982), p. 34.]
- ²¹F. Glas, *J. Appl. Phys.* **62**, 3201 (1987).
- ²²T. Kato, T. Matsumoto, M. Hosoki, and T. Ishida, *Jpn. J. Appl. Phys., Part 2* **26**, L1597 (1987).